X-Ray and Debris Emission from Direct and Indirect National Ignition Facility Targets

R.R. Peterson, J.J. MacFarlane, Ping Wang

May 1996

UWFDM-1016

Presented at the 12th Topical Meeting on the Technology of Fusion Power, 16–20 June 1996, Reno NV.

FUSION TECHNOLOGY INSTITUTE

UNIVERSITY OF WISCONSIN

MADISON WISCONSIN

X-Ray and Debris Emission from Direct and Indirect National Ignition Facility Targets

R.R. Peterson, J.J. MacFarlane, Ping Wang

Fusion Technology Institute
University of Wisconsin
1500 Engineering Drive
Madison, WI 53706

http://fti.neep.wisc.edu

May 1996

UWFDM-1016

Presented at the 12th Topical Meeting on the Technology of Fusion Power, 16–20 June 1996, Reno NV.

X-RAY AND DEBRIS EMISSION FROM DIRECT AND INDIRECT NATIONAL IGNITION FACILITY TARGETS

Robert R. Peterson, Joseph J. MacFarlane, and Ping Wang
Fusion Technology Institute, University of Wisconsin-Madison
1500 Engineering Drive
Madison, WI 53706-1687
(608) 263-5646

ABSTRACT

The emission of x rays and debris ions by the National Ignition Facility direct and indirect targets are compared in this paper. In the indirect drive targets, the fuel capsule is surrounded by a gold case, which filters out all but the hardest x rays from the capsule and collides with the capsule debris, generating large amounts of colder x rays that leave the target through laser entrance holes. The direct drive targets have no such case, so the debris and x rays from the capsule are un-obscured. Computer simulations of both targets demonstrate these differences.

I. INTRODUCTION

The National Ignition Facility (NIF)[1] will be used to shoot a variety of targets including direct and indirect drive inertial fusion targets. For the design of the facility, it is important to have a reasonable knowledge of the x-ray and debris output from the target. Direct and indirect drive targets are very different in their design and the nature of the x-ray and debris emissions. The x-ray and debris spectra are used to calculate how the first wall of the NIF will respond to target emissions and to lead to a viable target chamber design.

Target emanations have been calculated for direct and indirect drive NIF targets. The x-ray spectra from direct and indirect drive NIF targets have been calculated with both LASNEX[2] and BUCKY.[3] These calculations represent an improvement over earlier calculations for indirect drive targets[4] in the use of improved equations-of-state and opacities and better modeling of the radiation transport and thermonuclear burn within the BUCKY code. The indirect drive NIF target has been studied in two dimensions with the LASNEX code, which shows the angular dependence of the x-rays and debris, while the earlier calculations were all in one dimension.

The results of the computer simulations show the differences in the target emissions between direct and indirect drive targets. The x rays from direct drive targets are very hard but only make up about 1% of the yield, while indirect drive targets have much softer spectra that make up about 19% of the yield. Direct drive targets are made of less mass than indirect drive targets and have much more debris energy, so they have a more energetic ion spectrum. Typically, direct drive targets emit 50 keV tritiums, 35 keV deuteriums and 3 MeV carbons. Indirect drive targets emit mostly gold at energies of a few 100 keV. Both x-ray and debris spectra are isotropic for direct drive and non-isotropic for indirect drive.

II. INDIRECT DRIVE EMISSION

The emission of x rays and debris by the NIF indirect drive target is due to the complicated interaction of several phenomena. Some x-ray emissions from the laser plasmas take place during the implosion phase. When the target burns, some hard x rays are emitted by the fuel capsule. The capsule then expands very rapidly and then collides with the hohlraum case. This collision generates a stagnated hot plasma that radiates x rays, some of which leave the target through the laser entrance holes. Finally, the target disassembles into debris.

One-dimensional BUCKY code simulations of radiative breakout of the NIF indirect target have been performed. These are one-dimensional simulations of

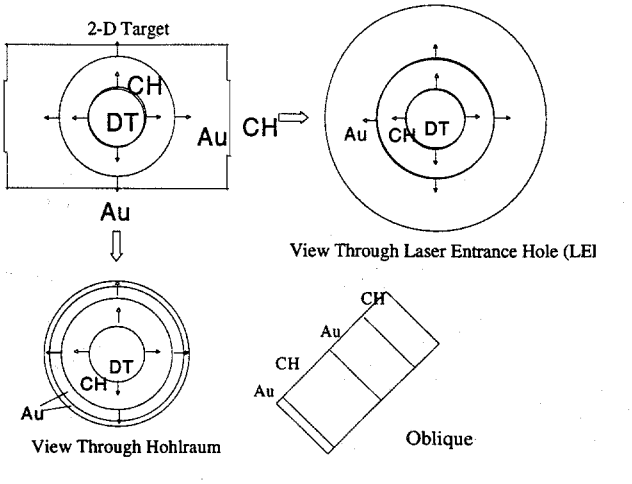

Fig. 1. One-dimensional simulations of the radiative breakup of the NIF indirect drive target.

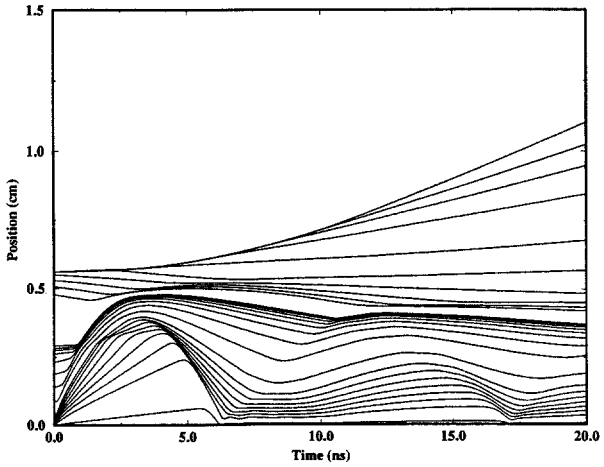

Fig. 2. Positions of Lagrangian zone boundaries for a BUCKY simulation of the radiative breakup of the NIF indirect drive target viewed "out through the case".

an inherently two dimensional process. Simulations have been performed in three directions; spherically out from the center of the capsule through the gold case, spherically out from the center of the capsule through the laser entrance hole, and from the back of the gold case at the point nearest the capsule out through the laser entrance hole in a slab geometry. The final calculation is called oblique. The three directions are depicted in Fig. 1.

No thermonuclear burn occurs in these simulations. It is assumed that burn has finished before the run starts. The burn energy is included in the initial energy in the capsule at the beginning of each run. The initial conditions (mass density, velocity, and temperatures) are obtained from the "out through case" run and the "laser entrance hole" run from profiles supplied by Jon Larsen,[5] which are results of a simulation with the HYADES[6] code. This calculation also neglected thermonuclear burn, but did model the implosion. The appropriate amounts of energy were added to these initial conditions by adjusting the temperature of the DT fuel. This procedure ignores the finite thermonuclear burn time and the transmutation of a fraction of the DT into helium. The first will tend to predict a higher than correct temperature for the DT plasma. The initial condition for the "out through the laser entrance hole case" is the same as in "out through the case", except the high mass density gold is excluded and a larger region of gold vapor is added. The initial conditions for the "oblique" run will be discussed later.

The BUCKY code used in these simulations has been used to study a variety of target chamber related physical phenomena, including laser and ion beam deposition, target implosion, thermonuclear burn, target microexplosions, fireballs in gases, and x-ray and debris ion response of structures in a target chamber. The hydrodynamic motion of the target plasma and the radiation released by the target are the issues of interest here. Hydrodynamic motion is calculated with a Lagrangian finite differencing scheme. Radiation transport is calculated here with multigroup flux limited diffusion, though BUCKY has options to transport individual lines or to use higher order multigroup methods. Equations-of-state and opacities are read in from tables generated by the EOSOPA[7] codes. The opacities are calculated with an unresolved transition array method for high atomic numbers, and a detailed configuration accounting method at low atomic number.

The plot of Lagrangian zone boundary positions from the "out through case" run are plots against time as seen in Fig. 2. One can clearly see the collision between the rapidly expanding capsule and the gold case that occurs at about 0.75 ns after the end of the burn. Near the collision time, the capsule plasma stagnates against the gold, heating the gold to several 100 eV. At the end of the run, the gold is at a velocity between 1.3×10^6 and 2.5×10^6 cm/s. The time-integrated spectrum leaving the back of the gold case

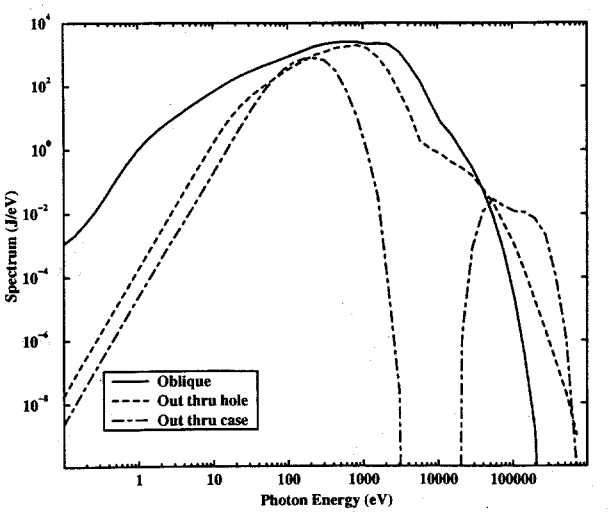

Fig. 3. Time-integrated x-ray spectrum from NIF indirect drive target when viewed "out through the case", "out through the hole", and in the "oblique" direction. From BUCKY simulations.

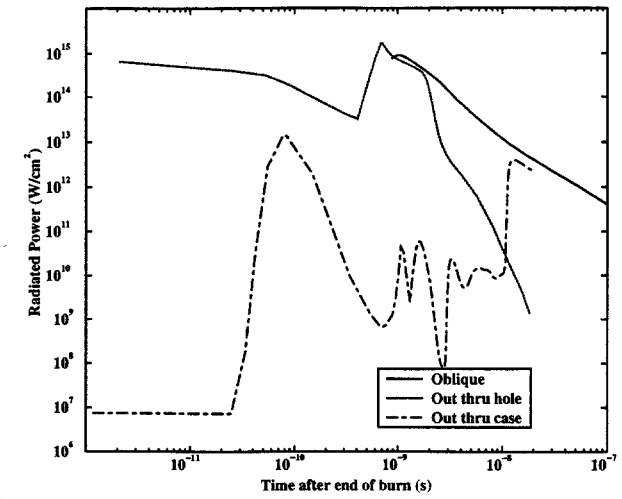

Fig. 4. NIF direct drive target design.

is shown in Fig. 3. The spectrum integrated out to the end of the run is approximately a blackbody spectrum at 200 eV.

In the "out through hole" run, one sees the rapidly expanding capsule with no impediment sweeping up the gold vapor in its path. At the end of the run the gold is at a velocity between 1.2×10^8 and 1.3×10^8 cm/s, and the DT and plastic velocities increase linearly with distance from the target. The time-integrated spectrum leaving the back of the gold vapor is shown in Fig. 3. The spectrum integrated out to the end of the run is approximately a blackbody spectrum at 330 eV.

The "oblique" run is a slab calculation with motion allowed at both boundaries. The initial conditions are taken from the "out through the case" run at peak stagnation. One sees the expanding high pressure stagnation region pushing the low pressure gold vapor in its path. The time-integrated spectrum leaving the laser entrance hole is shown in Fig. 3.

It is possible to estimate the angle dependent fluences of x-rays emitted by the target from a superposition of 1-D simulations. One could assume that the x rays burning through the case are isotropic and give some angle dependence to radiation leaving the LEH. But this would not induce truly 2-D effects that have been modeled with LASNEX. The fluence and the spectrum are seen to be very angle dependent, with the peak fluence observed between 15° and 30° from the hohlraum axis, which is where the oblique spectrum is dominant.

III. DIRECT DRIVE EMISSION

The x-ray and debris emission from a direct drive concept for a NIF target has been studied with LASNEX and BUCKY. The basic target concept is a pure solid DT inner shell with an outer plastic shell and the central void filled with DT vapor. The design is shown in Fig. 4. The laser pulse must be carefully shaped to implode this target. Chris Fontes at LANL has designed a laser pulse shape that implodes this target to ignition, generating about 40 MJ of yield. We have continued Fontes' LASNEX run[8] to the point in time when the target stops emitting x rays and the velocity profiles in the target stabilize. The emitted x-ray spectrum is hard (a blackbody spectrum of 1.7 keV). The LASNEX calculations predict a yield of about 40 MJ. We have used the BUCKY code to continue this study. BUCKY now has the capability to simulate laser deposition. The velocity, temperature and density profiles are shown in Fig. 5. From these profiles, we have deduced a target debris energy spectrum. The deuterium and tritium forms the peak in density at 2 cm. We have approximated the DT density profile as a Gaussian with a half width of 0.7 cm. The bump in density at 5 cm is due to the plastic

TABLE I

Direct Drive Target Debris Spectrum

Bin Number	1	2	3	4	5	6	7
Species	T	T	T	D	D	D	C
Velocity (cm/ns)	0.13	0.20	0.27	0.13	0.20	0.27	0.5
Energy (keV)	26.4	62.5	114	17.6	41.7	76	3130
Number of ions ($\times 10^{19}$)	4.77	12.3	4.77	4.77	12.3	4.77	.452
Start of pulse at 5 m (μs)	3.03	2.13	1.67	3.03	2.13	1.67	.980
End of pulse at 5 m (μs)	5.00	3.03	2.13	5.00	3.03	2.13	1.02
Pulse width at 5 m (μs)	1.97	0.9	0.46	1.97	0.9	0.46	0.04
Pulse energy (MJ)	0.202	1.30	0.871	0.135	0.865	0.58	2.26
Power (TW)	0.103	1.44	1.89	0.069	0.961	1.26	56.5

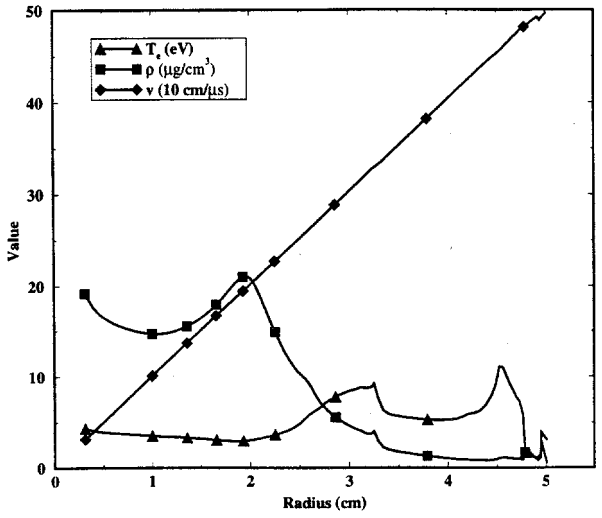

Fig. 5. Velocity, mass density, and plasma temperature profiles 10 ns after the end of burn for the NIF direct drive target with a 40 MJ yield. From a BUCKY simulation.

ablator. The velocity profile is linear in position and peaks at 0.5 cm/ns at 5 cm from the original center of the target.

From these profiles we have generated a discrete energy spectrum. The spectrum is shown in Table I. The spectrum consists of seven energy bins, where each bin has a given species, particle energy and power. The time of arrival of the start and end of each ion bin is given 5 m from the target, the position of the NIF first wall. There is a great deal of time-of-flight spreading during the transit of ions from the target to the wall. The deuterium and tritium bins have particle energies in the few 10's of keV range and μs pulse widths, while the carbon bin contains 3.13 MeV with a 40 ns pulse width. The carbon bin contains by far the largest pulse energy and power. These results could be more accurate with a larger number of bins, but we need to improve our method of converting Fig. 5 into the information in Table II. The results using this discrete spectrum will give representative results, but not the final answer.

IV. COMPARISON OF DIRECT AND INDIRECT DRIVE

During the summer of 1995 a series of LASNEX calculations was performed at and supported by Los Alamos National Laboratory to simulate the performance of direct and indirect drive NIF targets. Because of the relevance of these calculations to the NIF work discussed in this report, these results are summarized here. Details of these simulations will not be discussed. The energy balance of direct and indirect drive NIF targets are compared in Table II. Two types of direct drive targets are shown; one of pure DT and one with an outer plastic coating. Two indirect drive targets are also shown; one that barely ignited and one that experienced significant burn. The two direct drive targets performed in a very similar way. The direct drive x rays were all very hard (1.8 keV blackbody spectrum), though only 1% of the yield was in x rays. 19% of the direct drive yield was in debris and the rest in neutrons. The low fraction of energy in x rays is because most of the target is fully ionized after the end of the burn, so Bremsstrahlung is the dominant radiative emission process. The indirect drive targets have a much larger fraction of energy in x rays because the debris energy coming out of the capsule is converted into x rays by the collision between the capsule debris and the hohlraum case. The indirect drive

TABLE II

Target Energy Balance

	Direct Drive		Indirect Drive	
	Pure DT	CH Coated	Ignited	Significant Yield
E_{laser}	1.26	1.27	1.31	1.33
TN yield (MJ)	38.6	39.7	0.11	9.40
Neutron losses (MJ)	32.4	33.1	0.08	7.12
X-ray losses (MJ)	0.38	0.40	0.45	1.98
Debris energy (MJ)	7.04	7.44	0.89	1.63
Maximum total energy (MJ)	39.8	41.0	1.42	10.73

spectra are much cooler than the direct drive spectra because the stagnation region between the capsule and case is much cooler than the DT core during burn. The spectra and the fluence is very angle dependent. The x rays are mostly emitted from the stagnant gold plasma inside the hohlraum. The fact that some emission is seen even 90% off of the hohlraum axis is due to some of the hot gold plasma inside the case moving through the laser entrance holes. This angle dependence is a major difference between the direct and indirect drive NIF targets.

V. CONCLUSIONS

The x-ray and debris emissions are much different for the NIF direct and indirect drive targets. Because of the collision between the capsule and the case, the indirect drive target emits much more x-ray and less debris energy per shot than the direct drive target. The direct drive emissions are isotropic, while indirect drive targets emit with angle dependence. The emissions from direct drive targets have much harder x-ray and debris spectra.

ACKNOWLEDGEMENT

This work is supported by Lawrence Livermore National Laboratory and Los Alamos National Laboratory.

REFERENCES

1. M. Tobin, et al., "Target Area Design Basis and System Performance for the National Ignition Facility," *Fusion Technology* **26**, 772 (1994).

2. "LASNEX and Atomic Theory," LLNL Laser Program Annual Report 1980, Vol. 2, UCRL-50021-80.

3. J. J. MacFarlane, G. A. Moses, and R. R. Peterson, "BUCKY-1 – A 1-D Radiation Hydrodynamics Code for Simulating Inertial Confinement Fusion High Energy Density Plasmas," University of Wisconsin Fusion Technology Institute Report UWFDM-984 (August 1995).

4. R. R. Peterson, et al., "X-Ray and Debris Ion Spectra Emanating from NIF Targets," *Fusion Technology* **26**, 780 (1994).

5. Jon Larsen, Cascade Scientific Inc., private communication, (1995).

6. J. Larsen, "HYADES Users' Guide," Cascade Applied Sciences, Inc. Report CAS044 (May 1995).

7. P. Wang, "EOSOPA - A Code for Computing the Equations of State and Opacities of High Temperature Plasmas with Detailed Atomic Models," University of Wisconsin Fusion Technology Institute Report UWFDM-933 (December 1993).

8. C. Fontes, Los Alamos National Laboratory, private communication.